Chapter 1
Statistical Analysis Of Caustic Crossings In Multiply Imaged Quasars

Mediavilla, T., Ariza, O., Mediavilla, E., Alvarez, P.

Abstract Comparison between microlensing on quasars observed and simulated allow to infer conclusions about physical parameters such as source size, quasar brightness profile, mass distribution of the lens, abundance and mass of microlenses, and relative transverse velocity between source and lens. By simulating magnification maps for different values of the parameters we intend to calculate the probability that a variable takes a particular value. One of the problems facing this statistical study is that experimental errors and sources of variability other than microlensing can significantly affect data and results. To minimize this problem, we reduce the phenomenon of microlensing to a series of discrete events, the caustic crossings. If the source size is small (X-ray emitting source) each caustic crossing appears well resolved, would be of great amplitude (unaffected by measurement errors) and would be difficult to confuse with other types of variability. From the simulations we have calculated the probability that we are faced with a given distribution of mass in stars from the number of observed caustic crossings. We apply this study to the case of the image D of quasar QSO $2237 + 0305$.

Teresa Mediavilla
Universidad de Cadiz, Avda. Ramn Puyol, s/n,11202 e-mail: teresa.mediavilla@uca.es

Octavio Ariza
Universidad de Cdiz, Avda. Ramn Puyol, s/n,11202 e-mail: ocatvio.ariza@uca.es

Evencio Mediavilla
Universidad de La Laguna, Avda. Astrofisico Fco. Sanchez s/n, 38200 e-mail: emg@iac.es

Pilar Alvarez
Universidad de Cdiz, Avda. Ramn Puyol, s/n,11202 e-mail: pilar.ruiz@uca.es

1.1 Introduction

Although gravitational lensing is the term most used by astronomers to describe this phenomenon, the expression gravitational mirage is closer to its nature.

Terrestrial mirages are phenomena produced by the bending of light in the atmosphere due to variations in refractive index resulting from changes in temperature.

Not only variation in refractive index in the atmosphere causes the bending of light rays, but, as revealed in the 1919 eclipse experiment, gravity blends light rays too.

In the Solar System we can observe a weak effect of blending of light by gravity of sun, the variation in the apparent position of a star. But in other cosmological scenarios gravity can lead to a strong effect of curvature of light forming multiple images from a single source.

The object of our study is the deflection of light rays from a quasar, a bright source located in the depths of Universe, by the gravitational field of a galaxy almost aligned with quasar and observer. If there were no gravity, the ray would not be bent and observer would see the galaxy and a single source image. When gravity is present, paths of light ray are bent and light can follow more than one way to reach observer who can see more than one image of source. Then the observer would see galaxy and several quasar images around it.

We are interested in studying the quasar $2237+0305$, Einstein´s Cross. It is a multiple image system. The four images can be seen through the center of the galaxy where density of matter is greater. This causes the microlensing phenomenon what is the aim of our study.

In the scenario we are considering a galaxy acts as a lens to produce two images of a distant object, quasar. So far we have assumed the mass distribution of the galaxy is continuous, but in fact, the mass of the galaxy is discretely distributed in stars. the beam of light from one of the images may meet with a star that will act as a lens. We cannot see the images generated by this microlens because masses of stars are very small, and images cannot be

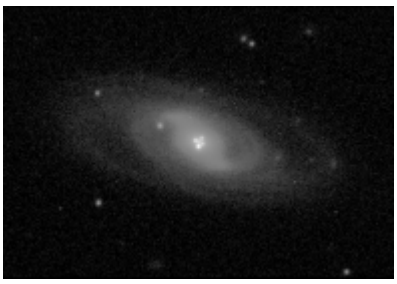

Fig. 1.1 QSO 2237+0305, Einstein´s Cross

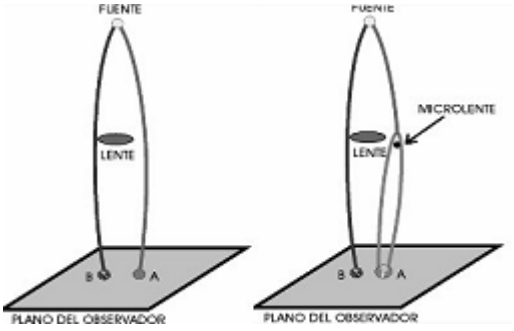

Fig. 1.2 Microlensing

separated with current measurement methods. However, microlenses produce an observable effect: magnification of image flux.

A sketch of lensing can be seen in Fig. 1.3. On the right we have source plane and on the left, lens plane (image plane). Lensing associates in general more than one image to a given source. Magnification is defined as the sum of the fluxes of all the images divided by source flux.

$$\mu = \sum_i \frac{F_{I_i}}{F_S} \ , \tag{1.1}$$

Liouville´s Theorem establishes fluxes are proportional to areas, then Eq. 1.1 is now written:

$$\mu = \sum_i \frac{S_{I_i}}{S} \ , \tag{1.2}$$

With this formulae we can calculate magnification of a given source in a given position in source plane. However, in most cases we would like to obtain light curves, that is to study changes in magnification when position of source changes or to study changes in magnification when parameters of source

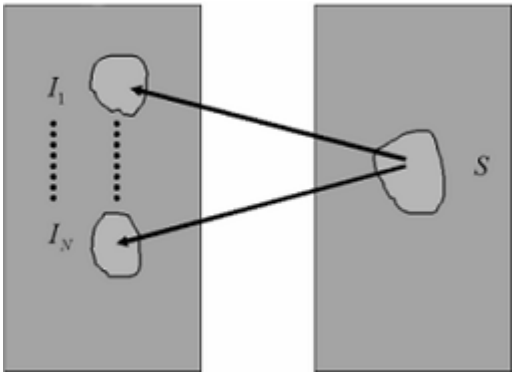

Fig. 1.3 Sketch of lensing

change, for instance the source size. To separate computation of magnification from source properties and position we can divide source plane in pixels. And compute magnification of each pixel. Then magnification of a source will be obtained as the convolution of its brightness with the magnification of pixels covered by the source. Thus, our objective is to calculate magnification maps, that is, magnification at each pixel in source plane. We have reduced our problem to compute the magnification of a pixel source of constant intensity. For this we need to evaluate source flux and images fluxes. That is, we need to find out all the images of the source. We need to solve lens equation which can be very difficult.

This is lens equation:

$$\overrightarrow{y} = \overrightarrow{x} - \overrightarrow{\alpha}(\overrightarrow{x}) \, , \tag{1.3}$$

A point in source plane has several images , so is one to many correspondence, and it is not a map. Solve lens equation is not always possible analytically and very difficult in other cases. On the other hand, inverse lens mapping is single-valuated, we can use it to obtain a source position for each point in image plane.

Some examples of magnification map are:

- Point-like lens magnification map:
  It is the simplest case. Magnification increases from outside to inside and reaches its maximum at center. This is a singular point because it cancels Jacobian and magnification is theoretically infinite. The geometrical place in source plane where Jacobian cancels is called caustic curve. In this case is degenerated at a point.
- Binary lens magnification map:
  In this case caustic curve is not degenerated. It has diamond shape
- If we add more lens, magnification map will be more complicated. It will have more and more caustic curves.

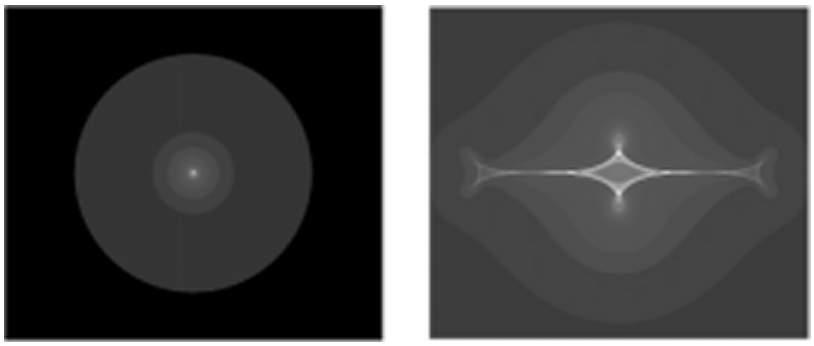

Fig. 1.4 Point-like lens magnification map (left). Binary magnification map (right)

1.1.1 Motivation and objectives

Fluctuations induced by microlensing in the observed light curves of quasars contain information about lensing objects (masses, density), about the unresolved source structure, and about the lens system (transversal velocity). So from a comparison between observed and simulated quasar microlensing we can obtain information about the physical parameters of interest. These conclusions can only be done in an statistical sense[1]. Thus, simulating magnification maps for some values of physical parameters we can try to calculate the probability that microlensing magnification takes a value determined from observations. This statistical analysis faces a problem: experimental errors and sources of variability other than microlensing can significantly affect data and results. To solve this problem we propose to simplify it reducing the microlensing effect to a series of discrete events, caustic crossings. If source size is small enough (X-ray emitting source)each caustic crossing will appear as a single event. In addition, caustic crossings are events of high magnification (little affected by measurement errors), and they are difficult to mistake with other kind of variability.

1.2 Statistical analysis of caustics concentration based on caustic crossings counts

We see a magnification map in Fig. 1.5. The straight line corresponds to the path of a pixel size source. On the right it is represented source´s light curve. Whenever source crosses a caustic a large increase in magnification that only can be associated with the phenomenon of caustic crossing is produced. That is, for a source of this size the light curve would provide direct information of an observable very interesting from an statistical point of view: the number

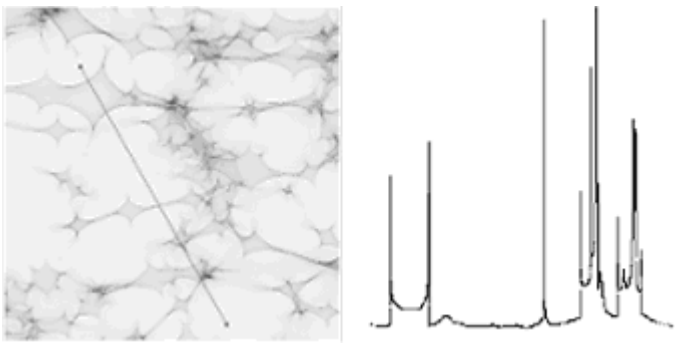

Fig. 1.5 Magnification map crossed by a source (left). Light curve of one pixel source (right)

of caustic crossings. One source of this size corresponds, in practice, to X-ray emission. However,if source were larger, it wouldn't be possible to identify caustic crossings as isolated events.

Distribution of caustics in magnification maps depends on the characteristics of star and dark matter distributions in lensing galaxy. In this work, we study how the existence of a range of masses in stars distribution affects to caustics concentration.

Statistical analysis of caustics spatial distribution is based on following steps:

1. Simulate magnification maps for different densities of matter and different mass distributions.
2. Identify caustic curves.
3. Count the number of caustics detected in a one-dimensional window of certain size in pixels for each axis.
4. Estimate probability of detecting a caustic in a pixel for each axis.
5. Compare experimental distributions obtained in simulations with theoretical binomial distribution.

We have used Inverse Polygon Mapping [2] to carry out steps 1 y 2.

1.3 Application to QSO 2237+0305

We have simulated magnification and caustics maps for the four images of QSO 2237+0305. We have considered two extreme cases in stars mass distribution: masses distributed in a range of masses (from 0.01 to 1 solar masses with a density law of $\frac{1}{m}$)(hypothesis I) and simple distribution of identical stars of one solar mass (hypothesis II).

We have counted the number of caustics detected in one-dimensional windows of 4, 40, 200 and 400 pixels for each axis and we have calculated experimental and theoretical binomial probability distributions. Comparing both distributions Fig. 1.6 we have obtained the following results:

- Differences between probability distributions are very significant in the case of image D. For example in X axis peak and centroid are between 6 and 7 detections when stars are distributed in a range and they are in one detection in unimodal case, in a 400 pixels size window.These parameters are in 3 detections when stars are distributed in a range and they are in zero in unimodal case, in a 200 pixels size windows. We have obtained similar results in Y axis.
- In the case of image D, from an experimental point of view, a single measure of the number of caustics detected in a window of 400 pixels would be sufficient to distinguish between hypotheses I and II. Let's assume that mean in X axis is 7 (expected value for I) and that error is

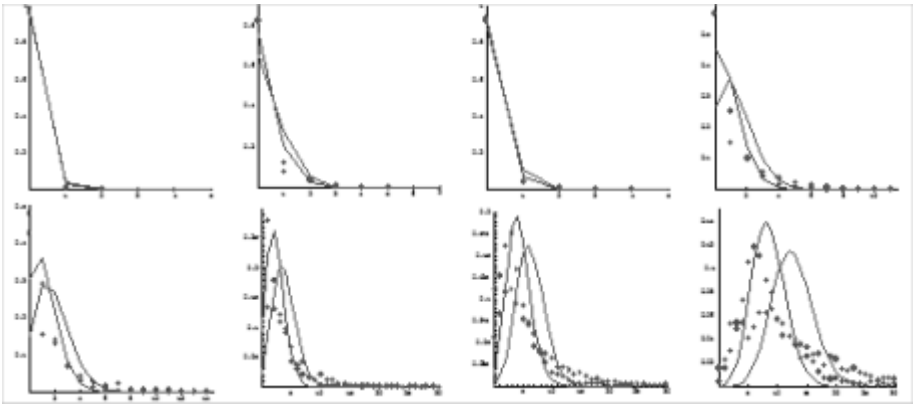

Fig. 1.6 Image D, comparisson between experimental (dotted line) and theoretical (continuous line) probability distributions in windows of 4, 40, 200 and 400 pixels. Columns first and second: hypothesis II, third and fourth: Hypothesis I.

± 3. P$(7 \pm 3/I)$=0.63 and P$(7 \pm 3/II)$=0.22. Applying Bayes´s Theorem and assuming that P(I) = P(II) we obtain p(I/7)=0.75 y P(II/7)=0.25. If we assume that mean is 1 ± 1 (expected value for II), P$(1 \pm 1/I)$=0.63 y P$(1 \pm 1/II)$=0.66, applying Bayes´s Theorem we will obtain P(I/1)=0.07 and P(II/1)=0.93. Let's assume that mean in Y axis is 10 ± 3(expected value for I), P$(10 \pm 3/I)$=0.37 and P$(10 \pm 3/II)$=0.12, applying Bayes´s Theorem we obtain P(I/10)=0.76 and P(II/10)=0.24. If the mean was 2 ± 1 (expected value for II), P$(2 \pm 1/I)$=0.12 and P$(2 \pm 1/II)$=0.38, applying Bayes´s Theorem we would obtain that P(I/2)=0.24 and P(II/2)=0.76.

- A general problem of studies on source flux variation due to microlensing is that we need to know the relative transverse velocity between the source and the microlenses. This amount is necessary in order to know experimental observation window size in suitable units (Einstein radii). Usually it is difficult to measure transversal velocity and the estimates of parameters depend on this magnitude in many experimental studies. In this case, obviously, the velocity of the source crossing magnification map will modify the number of caustic crossings in a window which size is expressed in pixels. The possibility of solve size/transversal velocity degeneracy depends on the case. In the image D, microlenses distributed in a range of masses, if the number of caustics (X axis) is greater than 6, the window will be grater than 1.2 Einstein radii, if the number of caustics (X axis) is less than 3, the window will be less than 1.2 Einstein radii, if the number of caustics (Y axis) is greater than 9, the window will be greater than 1.2 Einstein radii, if the number of caustics (Y axis) is less than 3, the window will be less than 1.2 Einstein radii.

We have constructed functions of probability conditioning to n caustic crossings for both hypothesis. From these and applying Bayes´s Theorem we

have obtained that probability of distinguishing between the two hypothesis with more than 80 percent of likelihood is 0.76 in a 400 pixels windows in X axis for D image. In Y axis probability of distinguishing between the two hypothesis with more than 70 percent of likelihood is 0.77.

1.4 Conclusions

- Caustic crossing statistics is affected by microlenses mass function and by shear.
- For D image of QSO 2237+0305 detection of a small number of events will allow us to distinguish between unimodal and distributed in a range mass distributions.
- We could determinate the size of observing window.

References

1. J. Wambsganss 1998 Gravitational lensing in Astronomy Liv. Rev. in Relavity , http://www.livingreviews.org/Articles/Volume1/1998-12wamb
2. E. Mediavilla, J. Muoz, P. Lopez, T. Mediavilla, C. Abajas, C. Gonzalez-Morcillo, Gil-Merino, 2006 ApJ 653 942-953.